PHYSICAL REVIEW D **95,** 115026 (2017)

Light Higgsinos, heavy gluino, and $b-\tau$ quasi-Yukawa unification: Prospects for finding the gluino at the LHC

Aditya Hebbar,[1,*] Qaisar Shafi,[1,†] and Cem Salih Ün[2,‡]

[1]*Bartol Research Institute, Department of Physics and Astronomy, University of Delaware, Newark, Delaware 19716, USA*

[2]*Department of Physics, Uludağ University, TR16059 Bursa, Turkey*

(Received 28 February 2017; published 22 June 2017)

A wide variety of unified models predict asymptotic relations at $M_{\rm GUT}$ between the b quark and τ lepton Yukawa couplings. Within the framework of supersymmetric $\mathrm{SU}(4)\times\mathrm{SU}(2)_L\times\mathrm{SU}(2)_R$, we explore regions of the parameter space that are compatible with b-τ quasi Yukawa Unification, Higgsinos being the lightest supersymmetric particles ($\lesssim$1 TeV) accompanied by a relatively low level of fine-tuning determined by the parameter $\Delta_{\rm EW}(\lesssim 200)$. Among the colored sparticles, the stop weighs more than 1.5 TeV or so, whereas the squarks of the first two families are significantly heavier, approaching 10 TeV in some cases. The gluino mass is estimated to lie in the 2–4 TeV range which raises the important question: Will the LHC find the gluino?

DOI: 10.1103/PhysRevD.95.115026

I. INTRODUCTION

Low scale supersymmetry (SUSY) remains an attractive extension of the standard model despite the apparent absence thus far of any direct experimental signature for its existence, or any new physics for that matter, at the LHC [1]. A supersymmetric scenario consisting of relatively light ($\lesssim$1 TeV Higgsinos) has attracted some attention in recent years [2,3]. It has been emphasized that this domain of supersymmetry may be more readily accessible at the much discussed ILC rather than at the LHC. The parameter space in this case has been referred to as "natural" SUSY [3], where the minimally supersymmetric standard model (MSSM) μ parameter and related parameters associated with radiative electroweak symmetry breaking (REWSB) are restricted to be comparable in magnitude to the Z-boson mass.

Our motivation in this paper is to realize a supersymmetric scenario with light Higgsinos within the framework of unified models that also displays approximate third family Yukawa coupling unification (YU). Well-known examples include approximate t-b-τ Yukawa unification [4,5] in SO(10) [6] and $\mathrm{SU}(4)\times\mathrm{SU}(2)_L\times\mathrm{SU}(2)_R$ (4-2-2) [7], and b-τ Yukawa unification which can occur in SO(10), 4-2-2 and SU(5) models. t-b-τ YU requires that the two MSSM Higgs doublets (H_d and H_u) reside in the 10—plet of SO(10). However, to incorporate fermion masses and mixings, it is necessary to extend the Higgs sector by introducing additional Higgs fields in the (15,1,3) and/or the (15,1,1) representations of 4-2-2. This breaks exact Yukawa unification, but the deviation from Yukawa unification can be restricted to within 20%, and such a modified scheme is often referred to as quasi-Yukawa unification (QYU)[8,9]. If Higgs fields from the above two (and possibly other) representations are present, then the top quark Yukawa coupling, in particular, may receive large corrections and therefore no longer unify with the b-τ Yukawa couplings. This particular scenario, called b-τ QYU, will be the focus of our study in this work. Note that TeV scale supersymmetry plays a critical role via radiative corrections [10] in implementing approximate Yukawa unification at $\mathrm{M_{GUT}}$. This may be considered additional evidence in support of supersymmetric grand unified theories (GUTs) versus their nonsupersymmetric counterparts which do not possess such threshold corrections.

The supersymmetric 4-2-2 with left-right symmetry naturally allows for nonuniversality in the MSSM gaugino sector. Thus, we can write

$$M_1 = \frac{3}{5}M_2 + \frac{2}{5}M_3 \tag{1}$$

which is implied by LR symmetry and hypercharge composition:

$$M_R = M_L \equiv M_2, \qquad Y = \sqrt{\frac{3}{5}}I_{3R} + \sqrt{\frac{2}{5}}(B-L), \tag{2}$$

where M_1, M_2 and M_3 are the asymptotic soft supersymmetric breaking (SSB) gaugino masses for $U(1)_Y$, $SU(2)_L$ and $SU(3)_C$. For the scalar sector we work with the so-called nonuniversal Higgs model 2 (NUMH 2) structure in which the soft scalar masses associated with the sfermions and the two MSSM Higgs doublets are treated as independent parameters.

*adityah@udel.edu
†shafi@bartol.udel.edu
‡cemsalihun@uludag.edu.tr

In order to explore the parameter space compatible with quasi b-τ QYU and light Higgsino, we employ the fine-tuning parameter $\Delta_{\rm EW}$ defined in [3]

$$\Delta_{\rm EW} \equiv \max_i(C_i)/(M_Z^2/2), \tag{3}$$

where $C_{H_u} = |-m_{H_u}^2 \tan^2\beta/(\tan^2\beta - 1)|$, $C_{H_d} = |m_{H_d}^2/(\tan^2\beta - 1)|$ and $C_\mu = |-\mu^2|$, along with analogous definitions for $C_{\Sigma_u^u}(k)$ and $C_{\Sigma_d^d}(k)$, where Σ_u^u and Σ_d^d refer to loop corrections to the SSB masses of H_u and H_d respectively (for detailed calculation of these loop corrections, see [11]). We further constrain the parameter space by requiring that $\Delta_{\rm EW} \lesssim 200$. Note that this condition is compatible with the light Higgsino condition $\mu \lesssim 1$ TeV.

If the neutralino is required to be the lightest supersymmetric particle (LSP), then the range of $\Delta_{\rm EW}$ we have considered here will result in mostly Higgsino-like LSP. For smaller values of $\Delta_{\rm EW}$, say 25–50, a second dark matter component, such as an axion, is needed to satisfy the dark matter abundance reported by WMAP [12] and Planck [13]. Values close to the upper limit (where $\mu \sim 1$ TeV) yield solutions in which the Higgsino alone satisfies the observed dark matter relic abundance in the universe.

In our discussion, following previous work [9], we express QYU as follows:

$$y_t : y_b : y_\tau = |1 + C_t| : |1 - C_{b\tau}| : |1 + 3C_{b\tau}|, \tag{4}$$

where C_t measures deviation in y_t, while $C_{b\tau}$ measures the deviation of y_b and y_τ. The factor of 3 in Eq. (4) has its origin in the Clebsch-Gordon coefficient associated with the 15-dimensional $\mathrm{SU}(4)_C$ representation [8,14]. Note that C_t does not have to be related to $C_{b\tau}$. For definiteness, we restrict $C_{b\tau} \leq 0.2$ and $C_t \leq 2$.

The rest of the paper is organized as follows: In Sec. II we describe our scanning procedure and summarize the experimental constraints employed in our analysis. In Sec. III we discuss the regions in the fundamental parameter space which are compatible with QYU and the light Higgsino conditions. In Sec. IV we present the sparticle mass spectrum and its implications for fine-tuning and DM. Section V focuses on the implications for dark matter (DM) based on current results from direct detection experiments. Our conclusions are summarized in VI.

II. SCANNING PROCEDURE AND EXPERIMENTAL CONSTRAINTS

We employ the ISAJET 7.84 package [15] to perform random scans over the parameter space given below. In this package, the weak scale values of gauge and third generation Yukawa couplings are evolved to $M_{\rm GUT}$ via the MSSM renormalization group equations (RGEs) in the $\overline{\rm DR}$ regularization scheme. While g_1, the gauge coupling for the hypercharge interactions, is not one of the fundamental gauge couplings of $SU(4)_C \times SU(2)_L \times SU(2)_R$, it can be written as a linear combination of them according to Eq. (2), and hence, the gauge coupling unification condition requires g_1 to be equal to the other couplings. In this context, if one assumes that $SU(4)_C \times SU(2)_L \times SU(2)_R$ breaks to $SU(3)_C \times SU(2)_L \times U(1)_Y$ at a high scale close to $M_{\rm GUT}$, the threshold corrections received by the MSSM gauge couplings are negligible and hence the unification of the MSSM gauge couplings can be maintained. In such a unification scheme, the threshold corrections to the gauge coupling of the strong interactions can cause a small deviation in g_3 from strict unification, but these corrections are not more than about 3% [16]. Therefore we apply the unification condition as $g_1 = g_2 \approx g_3$. With the boundary conditions given at $M_{\rm GUT}$, all the SSB parameters, along with the gauge and Yukawa couplings, are evolved back to the weak scale M_Z.

In evaluating Yukawa couplings, the SUSY threshold corrections [17] are taken into account at the common scale $M_{\rm SUSY} = \sqrt{m_{\tilde{t}_L} m_{\tilde{t}_R}}$. The entire parameter set is iteratively run between M_Z and $M_{\rm GUT}$ using the full 2-loop RGEs until a stable solution is obtained. To better account for leading-log corrections, one-loop step-beta functions are adopted for gauge and Yukawa couplings, and the SSB parameters m_i are extracted from RGEs at appropriate scales $m_i = m_i(m_i)$. The RGE-improved 1-loop effective potential is minimized at an optimized scale $M_{\rm SUSY}$, which effectively accounts for the leading 2-loop corrections. Full 1-loop radiative corrections are incorporated for all sparticle masses.

The requirement of radiative electroweak symmetry breaking (REWSB) [18] puts an important theoretical constraint on the parameter space. Another important constraint comes from limits on the cosmological abundance of stable charged particles [19]. This excludes regions in the parameter space where charged SUSY particles, such as $\tilde{\tau}_1$ or $\tilde{t}_1$, become the LSP.

We have performed random scans for the following parameter space:

$$\begin{aligned} 0 &\leq m_0 \leq 20 \text{ TeV} \\ 0 &\leq M_2 \leq 5 \text{ TeV} \\ 0 &\leq M_3 \leq 5 \text{ TeV} \\ -3 &\leq A_0/m_0 \leq 3 \\ 2 &\leq \tan\beta \leq 60 \\ 0 &\leq m_{H_u} \leq 20 \text{ TeV} \\ 0 &\leq m_{H_d} \leq 20 \text{ TeV}, \end{aligned} \tag{5}$$

with $\mu > 0$ and $m_t = 173.3$ GeV [20]. Note that our results are not too sensitive to one or two sigma variation in the value of m_t [10]. We use $m_b^{\overline{\rm DR}} = 2.83$ GeV and $m_\tau^{\overline{\rm DR}} = 1.7463$ GeV, which are hard-coded into ISAJET.

TABLE I. Benchmark points consistent with the experimental constraints mentioned in Sec. II. All masses are given in GeV. All points involve essentially 100% Higgsino dark matter.

	Point 1	Point 2	Point 3	Point 4	Point 5
m_0	3074	2375	2057	2745	2133
M_1	3941	3607	3350	3557	3387
M_2	5845	5009	4536	5069	4545
M_3	1084	1504	1571	1289	1654
M_{H_d}	615	725	800	609	752
M_{H_u}	1759	2025	2054	2152	2121
$\tan\beta$	44.7	42.9	40.5	44.3	42.3
A_0/m_0	−0.57	−0.62	−0.66	−0.72	−0.65
μ	**212.3**	**333.9**	**472**	**699**	**786**
ΔEW	**9.8**	**27.4**	**48.8**	**109.6**	**137.5**
m_h	123.2	123.5	123.3	123.6	123.4
m_H	1895	1586	1639	1244	1447
m_A	1883	1576	1629	1236	1437
$m_{H^\pm}$	1897	1588	1642	1248	1450
$m_{\tilde{\chi}^0_{1,2}}$	**207.3**, **209.4**	**326.8**, **329.3**	**460.7**, **463.6**	**688.1**, **690.8**	**769.7**, **772.9**
$m_{\tilde{\chi}^0_{3,4}}$	1792, 4856	1629, 4138	1509, 3739	1614, 4206	1529, 3749
$m_{\tilde{\chi}^\pm_{1,2}}$	**215.7**, 4845	**338.2**, 4120	**475.1**, 3720	**706.2**, 4189	**789.5**, 3728
$m_{\tilde{g}}$	**2487**	**3291**	**3407**	**2884**	**3571**
$m_{\tilde{u}_{L,R}}$	5099, 3754	4719, 3713	4460, 3604	4740, 3706	4585, 3762
$m_{\tilde{t}_{1,2}}$	1584, 4189	1939, 3910	2002, 3728	1760, 3845	2171, 3823
$m_{\tilde{d}_{L,R}}$	5100, 3646	4720, 3616	4460, 3513	4740, 3606	4585, 3672
$m_{\tilde{b}_{1,2}}$	2788, 4231	2901, 3936	2923, 3748	2795, 3871	3031, 3838
$m_{\tilde{\nu}_{e,\mu}}$	4843	4005	3579	4262	3627
$m_{\tilde{\nu}_\tau}$	4582	3798	3407	4008	3432
$m_{\tilde{e}_{L,R}}$	4838, 3373	4002, 2684	3578, 2357	4258, 3002	3626, 2427
$m_{\tilde{\tau}_{1,2}}$	2447, 4560	1941, 3784	1744, 3397	2131, 3992	1742, 3423
σ_{SI}(pb)	0.66×10^{-10}	0.10×10^{-09}	0.14×10^{-09}	0.17×10^{-09}	0.23×10^{-09}
σ_{SD}(pb)	0.12×10^{-05}	0.78×10^{-06}	0.58×10^{-06}	0.28×10^{-06}	0.32×10^{-06}
Ωh^2	0.008	0.02	0.041	0.0914	0.113
$y_{t,b,\tau}(M_{\rm GUT})$	0.55, 0.30, 0.41	0.54, 0.30, 0.39	0.54, 0.28, 0.36	0.55, 0.32, 0.42	0.54, 0.30, 0.39
C	0.08	0.07	0.07	0.08	0.08

In scanning the parameter space, we employ the Metropolis-Hastings algorithm as described in [21]. The data points collected all satisfy the requirement of REWSB, with the neutralino being the LSP in each case. After collecting the data, we impose the mass bounds on all the particles [19] and use the IsaTools package to implement the following phenomenological constraints [22–24]:

$$m_h = 123\text{–}127\ \text{GeV} \tag{6}$$

$$m_{\tilde{g}} \geq 1.8\ \text{TeV} \tag{7}$$

$$0.8\times10^{-9} \leq \text{BR}(B_s \to \mu^+\mu^-) \leq 6.2\times10^{-9}(2\sigma) \tag{8}$$

$$2.99\times10^{-4} \leq \text{BR}(b \to s\gamma) \leq 3.87\times10^{-4}(2\sigma) \tag{9}$$

$$0.15 \leq \frac{\text{BR}(B_u \to \tau\nu_\tau)_{\rm MSSM}}{\text{BR}(B_u \to \tau\nu_\tau)_{\rm SM}} \leq 2.41(3\sigma) \tag{10}$$

$$0.0913 \leq \Omega_{\rm CDM}h^2 \leq 0.1363(5\sigma). \tag{11}$$

We emphasize the mass bounds on the Higgs boson [25,26], and the gluino [27], since the experiments at the Large Hadron Collider (LHC) have had a strong impact on the bounds on these particles. The rare B-meson decays have a strong impact on the parameter space, since the SM predictions are already in good agreement with the experimental results. We have applied the constraints from $\text{BR}(B_s \to \mu^+\mu^-)$ [28] and $\text{BR}(b \to s\gamma)$ [29] within 2σ uncertainty, while the MSSM predictions on $\text{BR}(B_u \to \tau\nu_\tau)$ are limited to within 3σ uncertainty [30].

Another strict constraint comes from the DM observables. Since the LSP is proposed as a candidate for DM, the regions in the fundamental parameter space which yield charged sparticles as LSP are excluded. Thus, we accept only those solutions for which one of the neutralinos is the lightest supersymmetric particle (LSP) without necessarily

saturating the 5σ dark matter relic abundance bound observed by WMAP9. This is due to the fact that we are primarily motivated by natural SUSY which we interpret to mean MSSM μ parameter $\lesssim$1 TeV. The LSP Higgsino in this case does not necessarily saturate the DM abundance. We should note that if one requires the solutions to yield LSP neutralino as a dark matter candidate, the bounds in Eq. (11) provide a very strict constraint, since the relic abundance of LSP neutralino is quite large and hence severely violates the WMAP and Planck constraints. In order to satisfy these constraints, one requires some coannihilation mechanism(s) which reduce the relic abundance of LSP neutralino. However, if such mechanisms exist, the Boltzmann equation for Ωh^2 becomes highly nonlinear, and it can only be solved by using a numerical approximation. Since the solution to the Bolzmann equation is of the exponential form, even a small uncertainty in the relevant parameters used in the solution causes a large uncertainty in the calculation of Ωh^2. Taking these uncertainties into consideration, we have assumed that both the WMAP and the Planck bounds yield very similar DM phenomenology. The impact of direct detection on the parameter space is discussed in Sec. V.

Finally, as far as the muon anomalous magnetic moment a_μ is concerned, we require that the solutions must be at least as consistent with the data as the standard model ($0 \leq \Delta a_\mu \leq 55.4 \times 10^{-10}$ [31]).

III. PARAMETER SPACE COMPATIBLE WITH QUASI-YUKAWA UNIFICATION

In this section we present the fundamental parameter space of $b-\tau$ QYU and discuss its impact on the low scale. We begin with a discussion on the status of $t-b-\tau$ QYU under the low fine-tuning condition. Figure 1 displays plots in $C_t - \Delta_{\rm EW}$ and $C_t/C_{b\tau} - \Delta_{\rm EW}$ planes. All points are consistent with radiative electroweak symmetry breaking and neutralino LSP condition. Blue points satisfy all experimental constraints and $\mu \lesssim 1$ TeV. Brown points form a subset of blue, and they are consistent with the bound on the relic abundance of neutralino LSP. The horizontal line in the $C_t - \Delta_{\rm EW}$ plane is set as an upper bound on the deviation in y_t from the exact Yukawa unification, while that in the $C_t/C_{b\tau} - \Delta_{\rm EW}$ plane indicates the regions where $C_t = C_{b\tau}$. If $t-b-\tau$ quasi-Yukawa unification (QYU) condition is applied at $M_{\rm GUT}$, it also constrains the deviation in y_t from the exact Yukawa unification such that $C_t \leq 0.2$. However, as seen from the $C_t - \Delta_{\rm EW}$, C_t barely reaches down to the 0.2 bound indicated by the horizontal line in the low fine-tuning region ($\Delta_{\rm EW} \leq 200$). In addition, the solutions compatible with $t-b-\tau$ QYU are required to yield $C_t = C_{b\tau}$, which cannot be satisfied in the low fine-tuning region as shown in the $C_t/C_{b\tau} - \Delta_{\rm EW}$ plot. Thus, the low fine-tuning condition excludes solutions which are compatible with $t-b-\tau$ QYU condition.

Figure 2 displays $C_{b\tau}$ vs. the fundamental parameters with plots in $C_{b\tau} - m_0$, $C_{b\tau} - M_2$, $C_{b\tau} - M_3$ and $C_{b\tau} - \tan\beta$ planes. All points are compatible with REWSB and neutralino LSP. Green points satisfy all experimental constraints. Blue points form a subset which is compatible with $\mu \lesssim 1$ TeV and $\Delta_{\rm EW} < 200$. Brown points are a subset of blue and represent solutions consistent with the WMAP bound on the relic abundance of the LSP neutralino. We do not apply $C_{b\tau} \leq 0.2$, but instead indicate this bound with a horizontal line. As seen from the $C_{b\tau} - m_0$, $C_{b\tau} - M_2$ and $C_{b\tau} - M_3$ plots, most of the solutions lie below the horizontal line at $C_{b\tau} = 0.2$ and hence, $b-\tau$ QYU is not a strong constraint on these parameters. The solutions with $M_3 \lesssim 800$ GeV are excluded by the LHC constraints. Similarly, the LHC constraints exclude solutions with $\tan\beta \lesssim 5$. The low fine-tuning condition provides additional restrictions such that $\tan\beta \gtrsim 30$.

We continue discussing the fundamental parameters in Fig. 3 with plots in $M_1 - \mu$, $M_2 - \mu$ planes, which represent the low scale values of these parameters. The color coding is the same as Fig. 2, except that the blue points now satisfy $C_{b\tau} < 0.2$ in addition to $\mu \lesssim 1$ TeV and

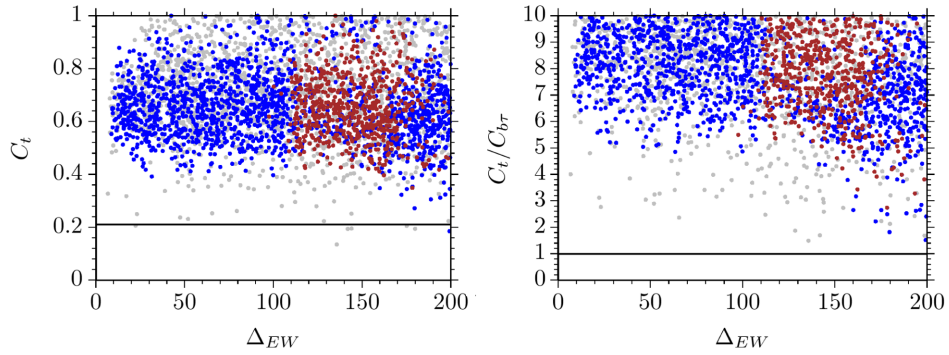

FIG. 1. Plots in $C_t - \Delta_{\rm EW}$ and $C_t/C_{b\tau} - \Delta_{\rm EW}$. All points are consistent with the radiative electroweak symmetry breaking and neutralino LSP condition. Blue points satisfy the LHC constraints and $\mu \leq 1$ TeV. Brown points form a subset of blue, and they are consistent with the bound on the relic abundance of neutralino LSP. The horizontal line in the $C_t - \Delta_{\rm EW}$ plane is set as an upper bound on the deviation in y_t from the exact Yukawa unification, while that in the $C_t/C_{b\tau} - \Delta_{\rm EW}$ indicates the regions for $C_t = C_{b\tau}$.

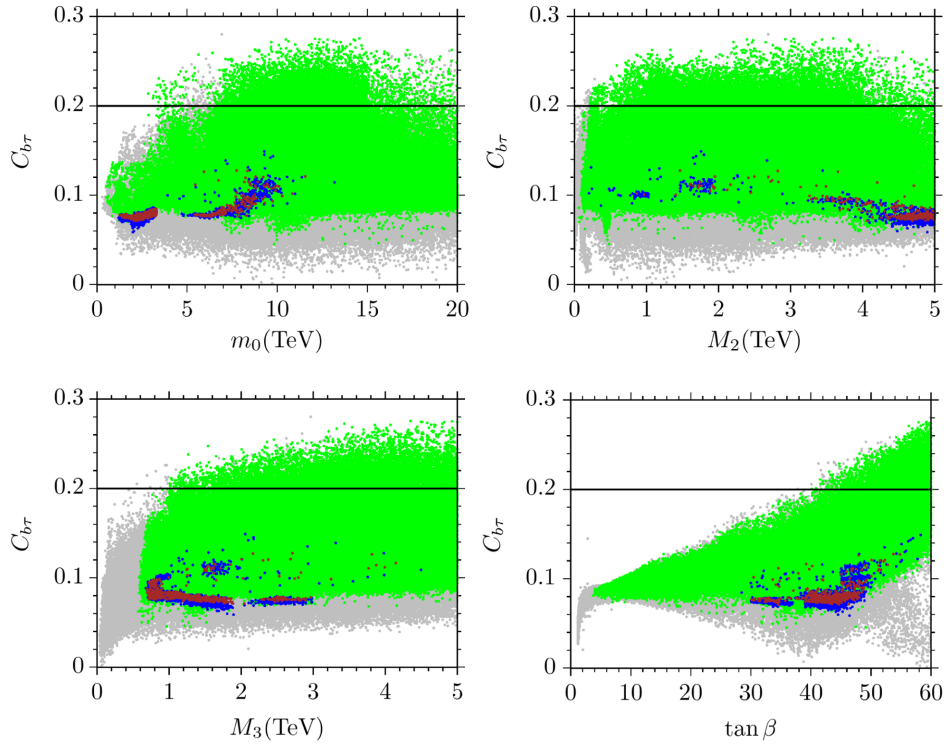

FIG. 2. Plots in the $C_{b\tau} - m_0$, $C_{b\tau} - M_2$, $C_{b\tau} - M_3$ and $C_{b\tau} - \tan\beta$ planes. All points are compatible with REWSB and neutralino LSP. Green points satisfy the experimental constraints. Blue points form a subset which is compatible with $b - \tau$ QYU, $\mu \lesssim 1$ TeV and $\Delta_{\rm EW} < 200$. Brown points are a subset of blue and represent solutions consistent with the WMAP bound.

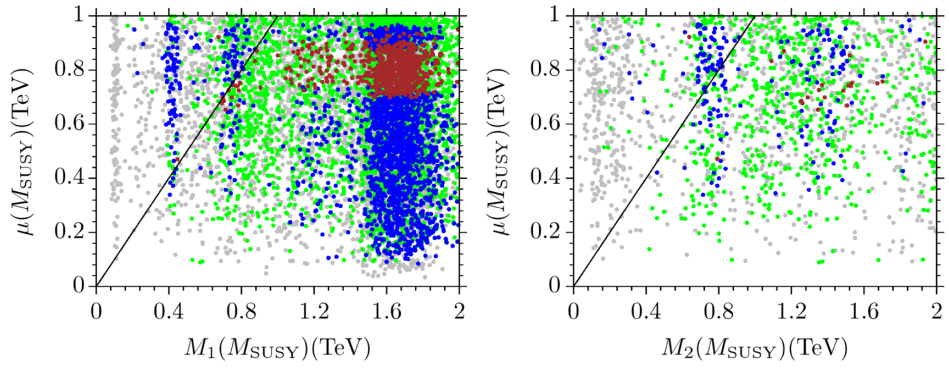

FIG. 3. Plots in the $M_1 - \mu$, $M_2 - \mu$ planes, which represent the low scale values of these parameters. Color coding is the same as in Fig. 2 except that the blue points now satisfy $C_{b\tau} \leq 0.2$ in addition to $\mu \lesssim 1$ TeV and $\Delta_{\rm EW} < 200$. The lines indicate the regions where $M_1 = \mu$ (left) and $M_2 = \mu$ (right).

$\Delta_{\rm EW} < 200$. These parameters simply show the masses of neutralinos at the low scale, since M_1 and M_2 are the SSB mass terms for bino and wino respectively, while μ determines masses of the Higgsinos. Except for a few points near the line in the two plots which indicate a Higgsino-bino or Higgsino-wino mixture dark matter, we see that for much of the parameter space, the dark matter is composed mainly of Higgsinos.

We next discuss fine-tuning through the $C_{b\tau} - \Delta_{\rm EW}$ and the $\Omega h^2 - \Delta_{\rm EW}$ plots in Fig. 4. The color coding is the same as Fig. 3. If dark matter is to be solely composed of Higgsinos, then the WMAP bound imposes a lower bound of $\sim$100 on $\Delta_{\rm EW}$, as seen from the $C_{b\tau} - \Delta_{\rm EW}$ plot. However, if we allow for multicomponent dark matter, then solutions with $\Delta_{\rm EW}$ as low as about 10 can also be found.

IV. SPARTICLE MASS SPECTRUM AND FINE-TUNING

In this section, we discuss the mass spectrum compatible with the $b - \tau$ QYU. Figure 5 displays plots in the

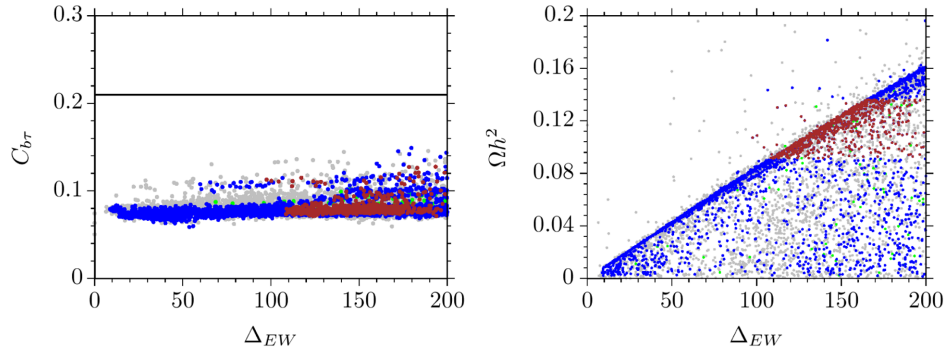

FIG. 4. Plots in the $C_{b\tau} - \Delta_{\rm EW}$ and the $\Omega h^2 - \Delta_{\rm EW}$ plane. Color coding is the same as Fig. 3.

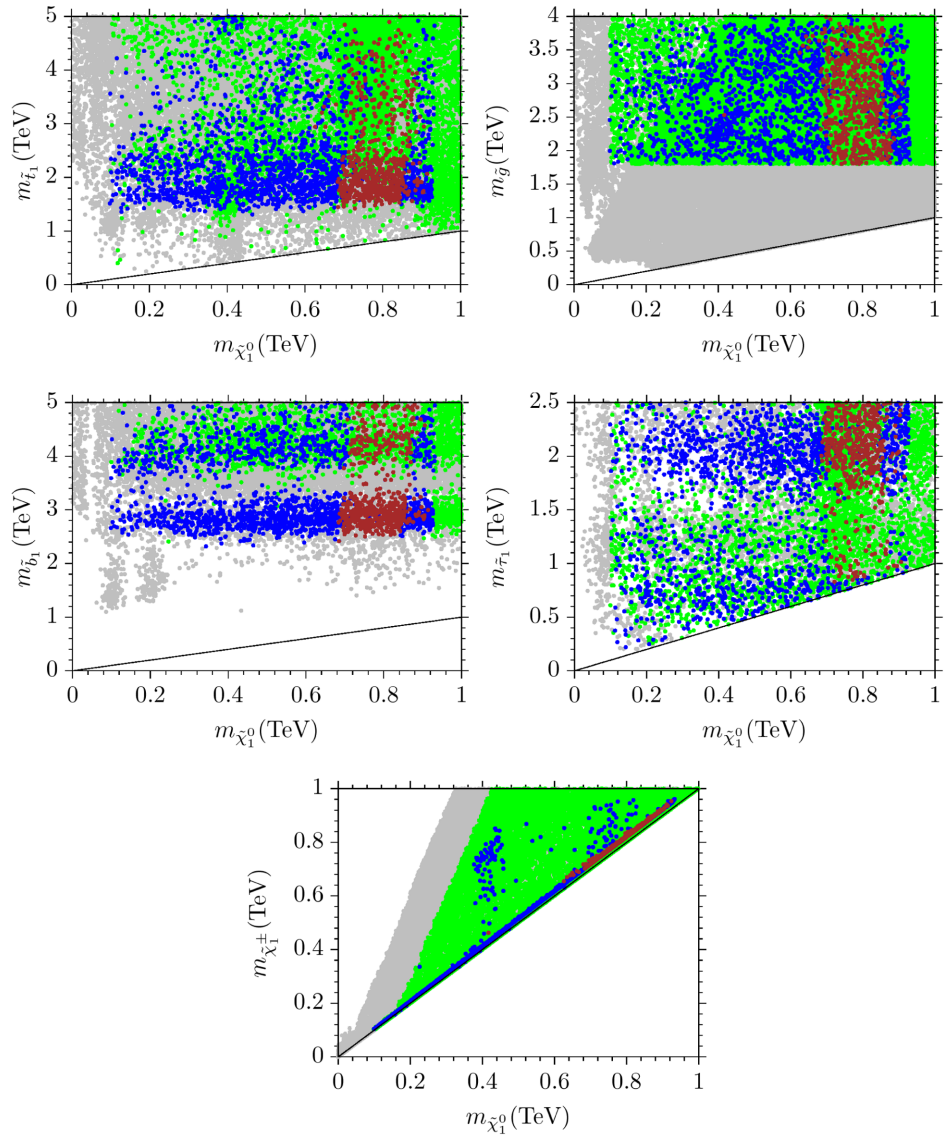

FIG. 5. Plots in the $m_{\tilde{t}_1} - m_{\tilde{\chi}_1^0}$, $m_{\tilde{g}} - m_{\tilde{\chi}_1^0}$, $m_{\tilde{b}_1} - m_{\tilde{\chi}_1^0}$, $m_{\tilde{\tau}_1} - m_{\tilde{\chi}_1^0}$ and $m_{\tilde{\chi}_1^\pm} - m_{\tilde{\chi}_1^0}$. Color coding is the same as in Fig. 3. The lines depict the regions where the sparticle and the LSP are nearly mass degenerate.

$m_{\tilde{t}_1} - m_{\tilde{\chi}_1^0}$, $m_{\tilde{g}} - m_{\tilde{\chi}_1^0}$, $m_{\tilde{b}_1} - m_{\tilde{\chi}_1^0}$, $m_{\tilde{\tau}_1} - m_{\tilde{\chi}_1^0}$ and $m_{\tilde{\chi}_1^\pm} - m_{\tilde{\chi}_1^0}$. Color coding is the same as in Fig. 3. The lines depict the regions where the sparticle and the LSP are nearly mass degenerate. We see that the mass of the stop quarks is $\gtrsim$1.5 TeV, while the gluino mass is bounded below by the current LHC lower bound of 1.8 TeV. The sbottom is heavier with mass $\gtrsim$2.5 TeV. We also show a plot of $m_{\tilde{\tau}_1}$ vs $m_{\tilde{\chi}_1^0}$, from which we note that there exist solutions with next-to-next-to-lightest supersymmetric particle (NNLSP) stau of mass as low as 200–250 GeV. The $m_{\tilde{\chi}_1^\pm} - m_{\tilde{\chi}_1^0}$ plane shows that the lightest chargino and LSP neutralino are nearly degenerate in mass. This result is not surprising, since the lightest chargino is also formed mostly by charged Higgsino, when the LSP neutralino is formed by the neutral Higgsinos. While their masses can be as low as about 100 GeV, the allowed range for the relic abundance of LSP neutralino bounds their masses as $m_{\tilde{\chi}_1^\pm} \sim m_{\tilde{\chi}_1^0} \gtrsim 700$ GeV.

We display plots between the lightest two colored supersymmetric particles, the stop and the gluino, and the fine-tuning parameter $\Delta_{\rm EW}$. The color coding is the same as in Fig. 3. We note that it is possible to have a gluino with mass ∼2–4 TeV for $\Delta_{\rm EW}$ as low as 30 or so [32]. We further observe that the stop mass can be as low as 1.5 TeV for the entire range of $\Delta_{\rm EW}$ that we consider. Experiments conducted at the LHC can probe gluino mass scales up to 2.8 TeV (for a detailed discussion see [32]). While this mass scale covers a part of our results, the null results for a gluino do not exclude the entire parameter space of natural SUSY. Hence, the next generation colliders will play a crucial role in the testability of our gluino results. In contrast to the gluino, the stop mass scale realized in our results is out of reach of the current experiments. The next generation of colliders can probe stop masses up to $m_{\tilde{t}} \sim 1.4$ TeV [33], which is still slightly below the mass scale shown in Fig. 6. In order to be consistent with the measured mass of the Higgs boson at the LHC, we require either a heavy stop, or large SSB trilinear scalar coupling or a suitable combination of the two. Large SSB trilinear scalar coupling, however, leads to higher fine-tuning [34].

V. HIGGSINO DARK MATTER AND DIRECT DETECTION

This section discusses the DM implications of $b-\tau$ QYU in the light of current and expected future results from the direct detection experiments. Figure 7 shows the results with plots in the $\sigma_{SI} - m_{\tilde{\chi}_1^0}$ and $\sigma_{SD} - m_{\tilde{\chi}_1^0}$ planes. The color coding is the same as in Fig. 3. In the $\sigma_{SI} - m_{\tilde{\chi}_1^0}$ plane, the dashed (solid) black line represents the current (future) results from the SuperCDMS experiment [35], and dashed (solid) red line(s) shows the current (future) results from the Xenon experiment [36]. The brown solid line is the latest result from the LUX experiment [37]. In the $\sigma_{SD} - m_{\tilde{\chi}_1^0}$ plane, the current upper bounds are set by Super-K [38] (red dashed line) and the IceCube DeepCore indicated by black dashed (solid) line for its current(future) results. In addition, the purple dashed line is the limit set by the CMS analyses [39], while the brown dashed line represents the latest result from the LUX experiment [40].

As can be seen from the $\sigma_{SI} - m_{\tilde{\chi}_1^0}$ plane, the DM scattering rate on nuclei yields relatively large cross-sections ($\sim 10^{-8}$ pb). These solutions involve Higgsino-like DM, and the large cross-section comes from the Yukawa interactions between the Higgsinos and quarks in nuclei. Although some of these solutions are excluded by the current results from the LUX experiment, they will be further tested by the SuperCDMS experiment. The penultimate solid red line represents the future results from Xenon 1T, which according to present plans, will be reached in 2017. The last solid red line is the projected result from the Xenon experiment over the next 20 years. The spin-dependent scattering results are shown in the $\sigma_{SD} - m_{\tilde{\chi}_1^0}$ plane, and all solutions are allowed by the current and future reaches of the experiments.

Finally, we present a table of six benchmark points, which exemplify our findings. The points chosen are consistent with the experimental constraints in Sec. II. The lowest value of $\Delta_{\rm EW}$ that we found was 9.6, with a LSP mass of 207 GeV, displayed in Point 1. Note that since the relic LSP density is about 10% of the desired DM

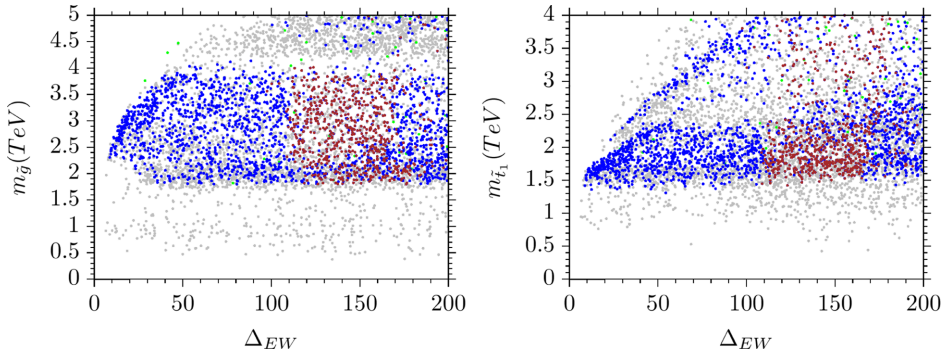

FIG. 6. Plots in the $m_{\tilde{g}} - \Delta_{\rm EW}$ and $m_{\tilde{t}_1} - \Delta_{\rm EW}$ planes. The color coding is the same as Fig. 3. The LHC lower bound on the gluino mass $m_{\tilde{g}} \geq 1.8$ TeV has been imposed.

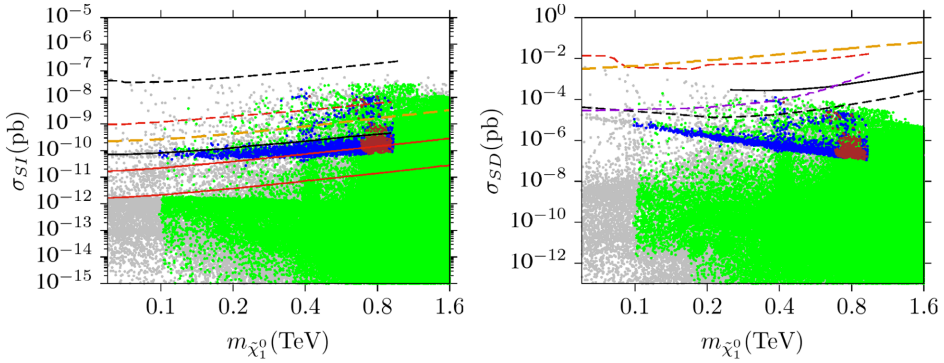

FIG. 7. Plots in the $\sigma_{SI} - m_{\tilde{\chi}_1^0}$ and $\sigma_{SD} - m_{\tilde{\chi}_1^0}$ planes. Color coding is the same as in Fig. 2. In the $\sigma_{SI} - m_{\tilde{\chi}_1^0}$ plane, the dashed (solid) black line represents the current (future) results from the SuperCDMS experiment [35], and dashed (solid) red line(s) shows the current (future) results from the Xenon experiment [36]. The brown solid line shows the latest result from the LUX experiment [37]. In the $\sigma_{SD} - m_{\tilde{\chi}_1^0}$ plane, the current upper bounds are set by the Super-K [38], indicated by the red dashed line, and the IceCube DeepCore by the black dashed (solid) line for its current and expected future results. In addition, the purple dashed line is the limit set by the CMS analysis [39], while the brown dashed line represents the latest results from the LUX experiment [40].

abundance, we posit that an additional DM component such as axion is also present. Points 2, 3 and 4 have progressively heavier LSPs which form a larger component of DM, but they require higher fine-tuning as measured by $\Delta_{\rm EW}$. Point 4 with an LSP mass of 688 GeV is the lightest higgsino DM compatible with the WMAP bound and we do not need any other dark matter component in this case. This point also corresponds to the lowest value of $\Delta_{\rm EW} \approx 110$ compatible with the WMAP bound for higgsino DM. Point 5 displays a pure Higgsino DM solution with the central value of relic density ($\Omega h^2 = 0.113$).

VI. CONCLUSION

We have explored how light ($\lesssim$1 TeV) Higgsinos can arise in supersymmetric $SU(4)_C \times SU(2)_L \times SU(2)_R$ models which exhibit quasi b-τ Yukawa unification. We also require that the electroweak fine tuning measure $\Delta_{\rm EW} \lesssim 200$. In the colored sector the stop mass is greater than 1.5 TeV or so. The first two family squarks are considerably heavier approaching 10 TeV in some cases. The gluino mass is estimated to lie in the 2–4 TeV range, which poses the important question: Will the LHC find the gluino?

ACKNOWLEDGMENTS

This work is supported in part by the DOE Grant No. DE-SC0013880 (A. H. and Q. S.), and the Scientific and Technological Research Council of Turkey (TUBITAK) Grant no. MFAG-114F461 (C. S. Ü.). This work used the Extreme Science and Engineering Discovery Environment (XSEDE), which is supported by the National Science Foundation grant number OCI-1053575. Part of the numerical calculations reported in this paper were performed at the National Academic Network and Information Center (ULAKBIM) of TUBITAK, High Performance and Grid Computing Center (TRUBA Resources).

[1] G. Aad *et al.* (ATLAS Collaboration), J. Instrum. **3**, P07007 (2008). S. Chatrchyan *et al.* (CMS Collaboration), J. Instrum. **3**, S08004 (2008).

[2] M. Drees, M. M. Nojiri, D. P. Roy, and Y. Yamada, Phys. Rev. D **56**, 276 (1997); **64**, 039901(E) (2001); K. Kowalska, L. Roszkowski, E. M. Sessolo, and S. Trojanowski, J. High Energy Phys. 04 (2014) 166; A. Mustafayev and X. Tata, Indian J. Phys. **88**, 991 (2014).

[3] H. Baer, V. Barger, P. Huang, A. Mustafayev, and X. Tata, Phys. Rev. Lett. **109**, 161802 (2012); H. Baer, V. Barger, P. Huang, D. Mickelson, A. Mustafayev, and X. Tata, Phys. Rev. D **87**, 035017 (2013); **87**, 115028 (2013).

[4] B. Ananthanarayan, G. Lazarides, and Q. Shafi, Phys. Rev. D **44**, 1613 (1991); Phys. Lett. B **300**, 245 (1993); Q. Shafi and B. Ananthanarayan, in *Trieste 1991, Proceedings, High energy physics and cosmology, vol. 1* (World Scientific, Singapore, 1991), p. 233.

[5] L. J. Hall, R. Rattazzi, and U. Sarid, Phys. Rev. D **50**, 7048 (1994); B. Ananthanarayan, Q. Shafi, and X. Wang, Phys. Rev. D **50**, 5980 (1994); R. Rattazzi and U. Sarid, Phys.

Rev. D **53**, 1553 (1996); T. Blazek, M. Carena, S. Raby, and C. Wagner, Phys. Rev. D **56**, 6919 (1997); J. L. Chkareuli and I. G. Gogoladze, Phys. Rev. D **58**, 055011 (1998); T. Blazek, S. Raby, and K. Tobe, Phys. Rev. D **62**, 055001 (2000); H. Baer, M. Brhlik, M. Diaz, J. Ferrandis, P. Mercadante, P. Quintana, and X. Tata, Phys. Rev. D **63**, 015007 (2000); C. Balazs and R. Dermisek, J. High Energy Phys. 06 (2003) 024; U. Chattopadhyay, A. Corsetti, and P. Nath, Phys. Rev. D **66**, 035003 (2002); T. Blazek, R. Dermisek, and S. Raby, Phys. Rev. Lett. **88**, 111804 (2002); M. Gomez, T. Ibrahim, P. Nath, and S. Skadhauge, Phys. Rev. D **72**, 095008 (2005); K. Tobe and J. D. Wells, Nucl. Phys. **B663**, 123 (2003); I. Gogoladze, Y. Mimura, and S. Nandi, Phys. Lett. B **562**, 307 (2003); W. Altmannshofer, D. Guadagnoli, S. Raby, and D. M. Straub, Phys. Lett. B **668**, 385 (2008); S. Antusch and M. Spinrath, Phys. Rev. D **78**, 075020 (2008); H. Baer, S. Kraml, and S. Sekmen, J. High Energy Phys. 09 (2009) 005; S. Antusch and M. Spinrath, Phys. Rev. D **79**, 095004 (2009); K. Choi, D. Guadagnoli, S. H. Im, and C. B. Park, J. High Energy Phys. 10 (2010) 025; M. Badziak, M. Olechowski, and S. Pokorski, J. High Energy Phys. 08 (2011) 147; S. Antusch, L. Calibbi, V. Maurer, M. Monaco, and M. Spinrath, Phys. Rev. D **85**, 035025 (2012).J. S. Gainer, R. Huo, and C. E. M. Wagner, J. High Energy Phys. 03 (2012) 097; H. Baer, S. Raza, and Q. Shafi, Phys. Lett. B **712**, 250 (2012); I. Gogoladze, Q. Shafi, and C. S. Un, J. High Energy Phys. 07 (2012) 055; M. Badziak, Mod. Phys. Lett. A **27**, 1230020 (2012); G. Elor, L. J. Hall, D. Pinner, and J. T. Ruderman, J. High Energy Phys. 10 (2012) 111; I. Gogoladze, Q. Shafi, and C. S. Un, Phys. Lett. B **704**, 201 (2011) J. High Energy Phys. 08 (2012) 028; S. Antusch, L. Calibbi, V. Maurer, M. Monaco, and M. Spinrath, Phys. Rev. D **85**, 035025 (2012); M. A. Ajaib, I. Gogoladze, and Q. Shafi, Phys. Rev. D **88**, 095019 (2013); M. Adeel Ajaib, I. Gogoladze, Q. Shafi, and C. S. Un, J. High Energy Phys. 07 (2013) 139; M. A. Ajaib, I. Gogoladze, Q. Shafi, and C. S. Un, arXiv:1308.4652.

[6] H. Georgi, in *AIP Conference Proceedings*, edited by C. Carlson (American Institute of Physics, New York, 1975), p. 575; H. Fritzsch and P. Minkowski, Ann. Phys. (N.Y.) **93**, 193 (1975).

[7] J. C. Pati and A. Salam, Phys. Rev. D **10**, 275 (1974).

[8] M. E. Gomez, G. Lazarides, and C. Pallis, Nucl. Phys. **B638**, 165 (2002).

[9] S. Dar, I. Gogoladze, Q. Shafi, and C. S. Un, Phys. Rev. D **84**, 085015 (2011); Q. Shafi, H. Tanyldz, and C. S. Un, Nucl. Phys. **B900**, 400 (2015).

[10] I. Gogoladze, R. Khalid, S. Raza, and Q. Shafi, J. High Energy Phys. 06 (2011) 117; I. Gogoladze, R. Khalid, and Q. Shafi, Phys. Rev. D **80**, 095016 (2009); I. Gogoladze, R. Khalid, S. Raza, and Q. Shafi, J. High Energy Phys. 12 (2010) 055.

[11] H. Baer, V. Barger, P. Huang, D. Mickelson, A. Mustafayev, and X. Tata, Phys. Rev. D **87**, 115028 (2013).

[12] G. Hinshaw *et al.* (WMAP Collaboration), Astrophys. J. Suppl. Ser. **208**, 19 (2013).

[13] P. A. R. Ade *et al.* (Planck Collaboration), Astron. Astrophys. **594**, A13 (2016).

[14] G. Lazarides, Q. Shafi, and C. Wetterich, Nucl. Phys. **B181**, 287 (1981).

[15] H. Baer, F. E. Paige, S. D. Protopopescu, and X. Tata, arXiv: hep-ph/0001086.

[16] J. Hisano, H. Murayama, and T. Yanagida, Nucl. Phys. **B402**, 46 (1993); Y. Yamada, Z. Phys. C **60**, 83 (1993); J. L. Chkareuli and I. G. Gogoladze, Phys. Rev. D **58**, 055011 (1998).

[17] D. M. Pierce, J. A. Bagger, K. T. Matchev, and R.-j. Zhang, Nucl. Phys. **B491**, 3 (1997).

[18] L. E. Ibanez and G. G. Ross, Phys. Lett. **110B**, 215 (1982); K. Inoue, A. Kakuto, H. Komatsu, and S. Takeshita, Prog. Theor. Phys. **68**, 927 (1982); **70**, 330(E) (1983); L. E. Ibanez, Phys. Lett. **118B**, 73 (1982); J. R. Ellis, D. V. Nanopoulos, and K. Tamvakis, Phys. Lett. **121B**, 123 (1983); L. Alvarez-Gaume, J. Polchinski, and M. B. Wise, Nucl. Phys. **B221**, 495 (1983).

[19] K. A. Olive *et al.* (Particle Data Group Collaboration), Chin. Phys. C **38**, 090001 (2014).

[20] (Tevatron Electroweak Working Group and CDF Collaboration and D0 Collab), arXiv:0903.2503.

[21] G. Belanger, F. Boudjema, A. Pukhov, and R. K. Singh, J. High Energy Phys. 11 (2009) 026; H. Baer, S. Kraml, S. Sekmen, and H. Summy, J. High Energy Phys. 03 (2008) 056.

[22] H. Baer and M. Brhlik, Phys. Rev. D **55**, 4463 (1997); H. Baer, M. Brhlik, D. Castano, and X. Tata, Phys. Rev. D **58**, 015007 (1998).

[23] K. Babu and C. Kolda, Phys. Rev. Lett. **84**, 228 (2000); A. Dedes, H. Dreiner, and U. Nierste, Phys. Rev. Lett. **87**, 251804 (2001); J. K. Mizukoshi, X. Tata, and Y. Wang, Phys. Rev. D **66**, 115003 (2002).

[24] D. Eriksson, F. Mahmoudi, and O. Stal, J. High Energy Phys. 11 (2008) 035.

[25] G. Aad *et al.* (ATLAS Collaboration), Phys. Lett. B **716**, 1 (2012).

[26] S. Chatrchyan *et al.* (CMS Collaboration), Phys. Lett. B **716**, 30 (2012).

[27] G. Aad *et al.* (ATLAS Collaboration), Phys. Lett. B **716**, 1 (2012).

[28] R. Aaij *et al.* (LHCb Collaboration), Phys. Rev. Lett. **110**, 021801 (2013).

[29] Y. Amhis *et al.* (Heavy Flavor Averaging Group Collaboration), arXiv:1207.1158.

[30] D. Asner *et al.* (Heavy Flavor Averaging Group Collaboration), arXiv:1010.1589.

[31] G. W. Bennett *et al.* (Muon g-2 Collaboration), Phys. Rev. D **73**, 072003 (2006).

[32] H. Baer, V. Barger, J. S. Gainer, P. Huang, M. Savoy, D. Sengupta, and X. Tata, arXiv:1612.00795; H. Baer, V. Barger, J. S. Gainer, P. Huang, M. Savoy, H. Serce, and X. Tata, arXiv:1702.06588, and references therein.

[33] Atlas Collaboration, Report No. ATL-PHYS-PUB-2014-010; (CMS Collaboration), arXiv:1307.7135.

[34] A. Cici, Z. Kirca, and C. S. Un, arXiv:1611.05270.
[35] P. L. Brink *et al.* (CDMS-II Collaboration), arXiv:astro-ph/0503583.
[36] E. Aprile *et al.* (XENON Collaboration), J. Cosmol. Astropart. Phys. 04 (2016) 027.
[37] D. S. Akerib *et al.*, Phys. Rev. Lett. **118**, 021303 (2017).
[38] T. Tanaka *et al.* (Super-Kamiokande Collaboration), Astrophys. J. **742**, 78 (2011).
[39] S. Chatrchyan *et al.* (CMS Collaboration), J. High Energy Phys. 09 (2012) 094; V. Khachatryan *et al.* (CMS Collaboration), Eur. Phys. J. C **75**, 235 (2015).
[40] D. S. Akerib *et al.* (LUX Collaboration), Phys. Rev. Lett. **116**, 161302 (2016).